

Insight into the Structure of Silver Cyanide from ^{13}C and ^{15}N Solid-State NMR SpectroscopyDavid L. Bryce^{†,‡} and Roderick E. Wasylshen^{*‡}*Department of Chemistry, Dalhousie University, Halifax, Nova Scotia, Canada B3H 4J3, and Department of Chemistry, University of Alberta, Edmonton, Alberta, Canada T6G 2G2*

Received February 25, 2002

The structure of silver cyanide has been investigated by solid-state multinuclear magnetic resonance spectroscopy. Carbon-13 and nitrogen-15 NMR spectra of magic-angle-spinning (MAS) and stationary powder samples of isotopically enriched Ag^{13}CN , $\text{Ag}^{13}\text{C}^{15}\text{N}$, and AgC^{15}N have been acquired at the external applied magnetic field strengths 4.7, 7.05, and 9.4 T. Axially symmetric carbon and nitrogen chemical shift (CS) tensors provide evidence for linearity of the polymeric $(-\text{Ag}-\text{CN}-)_n$ chains. A two-site model is required to successfully simulate the ^{13}C MAS NMR line shape, which is dominated by indirect nuclear spin–spin coupling between $^{109/107}\text{Ag}$ and ^{13}C nuclei. In combination with relativistic zeroth-order regular approximation density functional theory (ZORA-DFT) calculations on model AgCN fragments, the ^{13}C MAS NMR results show that $30 \pm 10\%$ of the silver sites are disordered, that is, either $-\text{NC}-\text{Ag}-\text{CN}-$ or $-\text{CN}-\text{Ag}-\text{NC}-$, and $70 \pm 10\%$ of the silver sites are ordered, that is, $-\text{NC}-\text{Ag}-\text{NC}-$. Effective dipolar coupling data extracted from ^{13}C NMR spectra of stationary samples allow an upper limit of 1.194 Å to be placed on the carbon–nitrogen internuclear distance. After incorporation of the effects of anisotropic indirect nuclear spin–spin coupling and motional averaging on the NMR-derived distance, a corrected value of $r_{\text{CN}} = 1.16 \pm 0.03$ Å is obtained. This work provides an example of the type of information which may be obtained from solid-state NMR studies of disordered materials and how such information may complement that available from diffraction studies.

Introduction

Applications of transition metal cyanides are widespread in chemistry, with recent interest in such diverse areas as molecular magnetism^{1–4} and the synthesis of porous supramolecular assemblies.^{5–12} Several recent papers have

examined specifically the chemistry of silver cyanides and gold cyanides,^{13–18} including the observation of strong photoluminescence in solutions of $\text{K}[\text{Au}(\text{CN})_2]$ and $\text{K}[\text{Ag}(\text{CN})_2]$.¹⁹ Cyano–silver and cyano–gold bonds are also

* Author to whom correspondence should be addressed. Telephone: 780-492-4336. Fax: 780-492-8231. E-mail: Roderick.Wasylshen@UAlberta.Ca.

[†] Dalhousie University.

[‡] University of Alberta.

- (1) Sokol, J. J.; Shores, M. P.; Long, J. R. *Angew. Chem., Int. Ed. Engl.* **2001**, *40*, 236–239.
- (2) Zhang, S.-W.; Fu, D.-G.; Sun, W.-Y.; Hu, Z.; Yu, K.-B.; Tang, W.-X. *Inorg. Chem.* **2000**, *39*, 1142–1146.
- (3) Vahrenkamp, H.; Geiss, A.; Richardson, G. N. *J. Chem. Soc., Dalton Trans.* **1997**, 3643–3651.
- (4) Vaucher, S.; Dujardin, E.; Lebeau, B.; Hall, S. R.; Mann, S. *Chem. Mater.* **2001**, *13*, 4408–4410.
- (5) Pfennig, B. W.; Fritchman, V. A.; Hayman, K. A. *Inorg. Chem.* **2001**, *40*, 255–263.
- (6) Bigozzi, C. A.; Argazzi, R.; Bortolini, O.; Scandola, F.; Harriman, A. *New J. Chem.* **1996**, *20*, 731–738.
- (7) Chesnut, D. J.; Plewak, D.; Zubieta, J. *J. Chem. Soc., Dalton Trans.* **2001**, 2567–2580.
- (8) Chesnut, D. J.; Kusnetzow, A.; Birge, R.; Zubieta, J. *Inorg. Chem.* **1999**, *38*, 5484–5494.

- (9) Haiduc, I.; Edelman, F. T. *Supramolecular Organometallic Chemistry*; Wiley-VCH: Weinheim, 1999; Chapter 4.
- (10) Iwamoto, T. In *Comprehensive Supramolecular Chemistry*; MacNicol, D. D., Toda, F., Bishop, R., Eds.; Pergamon Press: Oxford, 1996; Vol. 6, Chapter 19.
- (11) Shores, M. P.; Beauvais, L. G.; Long, J. R. *J. Am. Chem. Soc.* **1999**, *121*, 775–779.
- (12) Yuan, A.; Zou, J.; Li, B.; Zha, Z.; Duan, C.; Liu, Y.; Xu, Z.; Keizer, S. *Chem. Commun.* **2000**, 1297–1298.
- (13) Rawashdeh-Omary, M. A.; Omary, M. A.; Patterson, H. H. *J. Am. Chem. Soc.* **2000**, *122*, 10371–10380.
- (14) Guo, G.-C.; Wang, Q.-M.; Mak, T. C. W. *Inorg. Chem. Commun.* **2000**, *3*, 313–315.
- (15) Omary, M. A.; Webb, T. R.; Assefa, Z.; Shankle, G. E.; Patterson, H. H. *Inorg. Chem.* **1998**, *37*, 1380–1386.
- (16) Stein, T.; Lang, H. *Chem. Commun.* **2001**, 1502–1503.
- (17) Wang, Q.-M.; Mak, T. C. W. *J. Am. Chem. Soc.* **2001**, *123*, 1501–1502.
- (18) For a recent perspective on gold chemistry, see: Schmidbaur, H. *Nature* **2001**, *413*, 31–33.
- (19) Rawashdeh-Omary, M. A.; Omary, M. A.; Patterson, H. H.; Fackler, J. P., Jr. *J. Am. Chem. Soc.* **2001**, *123*, 11237–11247.

Table 1. Definition of Sites and Models Discussed for Silver Cyanide

	environment about Ag	model for the ZORA-DFT calculation of $^1J(^{109/107}\text{Ag}, ^{13}\text{C})$
ordered ^a	“-NC-Ag-NC-”	NC-Ag-NC-Ag (model I)
disordered ^b	“-NC-Ag-CN-” “-CN-Ag-NC-”	NC-Ag-CN-Ag (model II)

^a We define cyanide head-tail “order” as the case where all cyanide groups are oriented in the same direction within a given AgCN chain, i.e., in a parallel manner. Thus, in the case of a perfectly “ordered” silver cyanide chain, all silver atoms lie in sites of the type shown here, where Ag is bonded to one carbon atom and one nitrogen atom (see also model A in Table 4). ^b We define cyanide head-tail “disorder” as the case where there is not perfect parallel ordering of the cyanide groups within a given AgCN chain. Thus a “disordered” silver site refers to the situation shown here, where Ag is bonded to either two carbon atoms or two nitrogen atoms. We note that in the context of these definitions it is possible to have a perfectly “disordered” AgCN chain wherein the orientation of each cyanide moiety alternates with respect to its nearest neighbor, resulting in an antiparallel arrangement of cyanides. Nevertheless, this antiparallel arrangement is labeled as 100% disordered for the purposes of discussion (see model D in Table 4).

of importance in the self-assembled metal colloid monolayer approach to surface-enhanced Raman scattering experiments.²⁰

Interestingly, the structures of some “simple” inorganic compounds are not well understood, for example, silver cyanide, AgCN, and gold cyanide, AuCN. Only recently has the structure of solid copper cyanide been determined.²¹ Characterization of these prototypal transition metal complexes is of importance to provide a foundation for the understanding of more complex structures.

In 1999, Bowmaker et al. published powder neutron diffraction structures of AuCN and AgCN and found that both systems exist as “infinite” linear chains of alternating metal and cyanide moieties.²² Silver cyanide was found to be translationally disordered, with adjacent chains displaced along their long axis relative to each other. However, the possibility of so-called cyanide “head-tail” disorder, that is, -CN-Ag-CN- versus -NC-Ag-CN- versus -CN-Ag-NC- (see Table 1), was not addressed. In the present work, we define an ordered silver site to be one for which the two directly bonded cyanide groups are oriented in the same direction such that the silver atom is bonded to one carbon atom and one nitrogen atom. Similarly, a disordered silver site is defined as one which is bonded to either two carbon atoms or two nitrogen atoms (see Table 1).

In 2002, Hibble and co-workers²³ carried out a total neutron diffraction study of AgCN and reported bond lengths, $r_{\text{AgC}} = r_{\text{AgN}} = 2.06 \text{ \AA}$ and $r_{\text{CN}} = 1.16 \text{ \AA}$, which differ significantly from those determined by Bowmaker, $r_{\text{AgC}} = 2.15(6) \text{ \AA}$, $r_{\text{AgN}} = 1.86(8) \text{ \AA}$, and $r_{\text{CN}} = 1.26(9) \text{ \AA}$. The study of Hibble makes reference to the possibility of head-tail

disorder in AgCN, and their model correlation function, $T(r)$, incorporates the assumption of random ordering of the CN groups.

Hibble suggests that a nuclear magnetic resonance study of AgCN may be useful in providing additional information from a different perspective on the structure of AgCN, in particular the head-tail cyanide disorder. Solid-state NMR is indeed well-suited for probing disordered materials and has been applied to elucidate the structure and nature of the disorder in solid copper cyanide.²¹ Beneficial insights into the structure and bonding in several ordered, crystalline cyanometalates have also been provided by solid-state multinuclear magnetic resonance.^{24–27} Through the analysis of second-rank NMR interaction tensors such as chemical shift (CS) tensors, direct dipolar coupling tensors, and indirect nuclear spin-spin coupling tensors (**J**), the opportunity exists under favorable circumstances to provide information on molecular geometry, connectivity, and ordering in solid silver cyanide.

In the present work, we present a ¹³C and ¹⁵N solid-state NMR study of various isotopomers of silver cyanide: AgCN in natural abundance, Ag¹³CN (99%), Ag¹³C¹⁵N (99%), and AgC¹⁵N (99%). The study of several isotopomers at three different external applied magnetic field strengths will allow for a precise determination of several important NMR parameters which may be interpreted to provide information on the structure of silver cyanide. In particular, the present work endeavors to provide structural information which is complementary to the neutron diffraction studies, to resolve the discrepancy of 0.1 Å in the reported carbon-nitrogen bond lengths from these studies, and to provide a clearer picture of the nature of the disorder in silver cyanide.

Theory

There are five spin-active isotopes to consider when carrying out solid-state NMR spectroscopy of silver cyanide: ¹⁰⁹Ag ($I = 1/2$, NA = 48.18%), ¹⁰⁷Ag ($I = 1/2$, NA = 51.82%), ¹³C ($I = 1/2$, NA = 1.108%), ¹⁵N ($I = 1/2$, NA = 0.37%), and ¹⁴N ($I = 1$, NA = 99.63%). By selectively isotopically enriching the carbon and/or nitrogen sites, different and complementary information may be obtained from NMR experiments.

The NMR interactions of interest in the present work are the direct dipolar interaction, the indirect nuclear spin-spin (**J**) coupling interaction, and the chemical shift (CS) interaction. Each of these interactions has the ability to provide unique information on the structure of silver cyanide.

Direct Dipolar and Indirect Nuclear Spin-Spin Coupling Interactions. The direct dipolar coupling interaction is analogous to the classical magnetic interaction between two bar magnets and depends intimately on the motionally averaged inverse cube of the internuclear distance of the two coupled nuclei, $\langle r_{12}^{-3} \rangle$. This interaction is quantified by the

(20) Freeman, R. G.; Grabar, K. C.; Allison, K. J.; Bright, R. M.; Davis, J. A.; Guthrie, A. P.; Hommer, M. B.; Jackson, M. A.; Smith, P. C.; Walter, D. G.; Natan, M. J. *Science* **1995**, *267*, 1629–1632.

(21) Kroeker, S.; Wasylishen, R. E.; Hanna, J. V. *J. Am. Chem. Soc.* **1999**, *121*, 1582–1590.

(22) Bowmaker, G. A.; Kennedy, B. J.; Reid, J. C. *Inorg. Chem.* **1998**, *37*, 3968–3974.

(23) Hibble, S. J.; Cheyne, S. M.; Hannon, A. C.; Eversfield, S. G. *Inorg. Chem.* **2002**, *41*, 1042.

(24) Wu, G.; Kroeker, S.; Wasylishen, R. E. *Inorg. Chem.* **1995**, *34*, 1595–1598.

(25) Kroeker, S.; Wasylishen, R. E. *Can. J. Chem.* **1999**, *77*, 1962–1972.

(26) Wu, G.; Wasylishen, R. E. *J. Phys. Chem.* **1993**, *97*, 7863–7869.

(27) Kim, A. J.; Butler, L. G. *Inorg. Chem.* **1993**, *32*, 178–181.

direct dipolar coupling constant, R_{DD} :

$$R_{\text{DD}} = \frac{\mu_0 \gamma_1 \gamma_2 \hbar}{4\pi 2\pi} \langle r_{12}^{-3} \rangle \quad (1)$$

Here, γ_1 and γ_2 are the magnetogyric ratios of the coupled nuclei.

The **J** coupling interaction may be described as the sum of isotropic, J_{iso} , and anisotropic, ΔJ , parts. The isotropic coupling constant is well-known from solution NMR spectroscopy, where it manifests itself as a field-independent splitting. The Hamiltonian describing the anisotropic part of the **J** coupling tensor is identical in form to the Hamiltonian describing the direct dipolar interaction,²⁸ and as a result, the two interactions cannot be separated. This phenomenon is represented by the following equation,

$$R_{\text{eff}} = R_{\text{DD}} - \frac{\Delta J}{3} \quad (2)$$

where the *effective dipolar coupling constant*, R_{eff} , is the quantity which is measured experimentally. Thus, when attempting to extract internuclear distances from solid-state NMR experiments, two issues must be considered: (i) the magnitude of ΔJ and (ii) the extent to which motional averaging affects R_{DD} .

Chemical Shift Interaction. Typically the dominant NMR interaction in the spectra of spin- $1/2$ nuclei is the chemical shift (CS) interaction. The chemical shift interaction is properly described by a second-rank tensor. In its principal axis system, the symmetric part of the CS tensor may be described by three principal components, $\delta_{11} \geq \delta_{22} \geq \delta_{33}$. The isotropic chemical shift, δ_{iso} , is the average of these three components. It is also convenient to define two derived quantities, the span (Ω) and the skew (κ), which help in describing the CS tensor:

$$\Omega = \delta_{11} - \delta_{33} \quad (3)$$

$$\kappa = \frac{3(\delta_{22} - \delta_{\text{iso}})}{\Omega} \quad (4)$$

For an axially symmetric CS tensor, there are only two unique principal components which are commonly represented as δ_{\parallel} and δ_{\perp} . In such cases, $\kappa = \pm 1$.

Dipolar–Chemical Shift Method. For an isolated AX spin pair, the dipolar–CS method allows, under favorable conditions when symmetry dictates the orientation of one of the principal components of the CS tensor, for the determination of the effective dipolar coupling constant, the principal components of the CS tensor, and the orientation of the CS tensor with respect to the dipolar vector.^{29–36}

(28) Wasylishen, R. E. In *Encyclopedia of Nuclear Magnetic Resonance*; Grant, D. M., Harris, R. K., Eds.; Wiley Inc.: Chichester, UK, 1996; pp 1685–1695.

(29) Wasylishen, R. E.; Curtis, R. D.; Eichele, K.; Lumsden, M. D.; Penner, G. H.; Power, W. P.; Wu, G. In *Nuclear Magnetic Shieldings and Molecular Structure*; Tossell, J. A., Ed.; NATO ASI Series, Series C: Mathematical and Physical Sciences; Kluwer Academic Publishers: Dordrecht, 1993; Vol. 386, pp 297–314.

(30) VanderHart, D. L.; Gutowsky, H. S. *J. Chem. Phys.* **1968**, *49*, 261–271.

Considerable simplifications result for heteronuclear spin pairs in an axially symmetric environment,^{24,26,29,37} as is the case for the ^{13}C – ^{15}N spin pair in $\text{Ag}^{13}\text{C}^{15}\text{N}$; the effective dipolar coupling constant manifests itself as a readily measurable splitting in the stationary powder pattern.

Experimental and Computational Details

Sample Preparation. A typical synthesis of silver cyanide involved mixing equimolar amounts of silver nitrate (5.06 g, 29.8 mmol) and potassium cyanide (1.98 g, 30.4 mmol) dissolved in water. Upon mixing, silver cyanide precipitates immediately as a white powder. The product was collected by filtration, washed several times with water and ethanol, and dried on a high-vacuum line. For the natural-abundance sample, IR spectra (Nujol mull) were recorded, giving peaks at 2163 and 478 cm^{-1} , which have been assigned previously to C–N stretching and Ag–C bending modes, respectively.²² Preparations of ^{13}C - and ^{15}N -enriched samples, Ag^{13}CN (99%), AgC^{15}N (99%), and $\text{Ag}^{13}\text{C}^{15}\text{N}$ (99%), were carried out using the appropriate 99% isotopically enriched potassium cyanide.

Solid-State NMR Spectroscopy. Carbon-13 NMR spectra of solid $\text{Ag}^{13}\text{C}^{15}\text{N}$ (MAS and stationary) were acquired at 4.7 T ($\nu_{\text{L}}(^{13}\text{C}) = 50.33$ MHz) on a Chemagnetics CMX Infinity 200 spectrometer using a 5 mm (rotor o.d.) MAS probe, at 7.05 T ($\nu_{\text{L}}(^{13}\text{C}) = 75.43$ MHz) on a Bruker AM300 spectrometer using a 7 mm (rotor o.d.) MAS probe, and at 9.4 T ($\nu_{\text{L}}(^{13}\text{C}) = 100.6$ MHz) on a Bruker AMX400 spectrometer using a 4 mm (rotor o.d.) MAS probe. For all spectrometers, adamantane was used as an external ^{13}C reference, with peaks at 38.56 and 29.50 ppm relative to TMS. The magic angle was set by maximizing the number of rotational echoes in the ^{23}Na FID of solid sodium nitrate.³⁸ Carbon-13 $\pi/2$ pulse widths were approximately 5.0 μs on all spectrometers. In practice, shorter pulses (e.g., 2 μs) were used to acquire spectra of stationary samples in order to provide a more uniform and complete excitation of the powder pattern. Recycle delays were typically 100–200 s. A variety of MAS rates ranging from 2.1 to 7.6 kHz were employed. Carbon-13 NMR spectra of MAS and stationary samples of solid Ag^{13}CN were also acquired at 4.7 and 9.4 T.

Nitrogen-15 NMR spectra of solid AgC^{15}N and $\text{Ag}^{13}\text{C}^{15}\text{N}$ were acquired at 4.7 T ($\nu_{\text{L}}(^{15}\text{N}) = 20.29$ MHz) and 9.4 T ($\nu_{\text{L}}(^{15}\text{N}) = 40.6$ MHz) using the same 5 and 4 mm MAS probes described above. The ^{15}N ammonium resonance of solid $^{15}\text{NH}_4^{15}\text{NO}_3$ was used as an external reference and set to 23.8 ppm with respect to neat ammonia.³⁸ Nitrogen-15 labeled ammonium nitrate was also used to establish the ^{15}N $\pi/2$ pulse width as approximately 5.0 μs on both spectrometers. Recycle delays were 200–300 s. A variety of MAS rates ranging from 2.5 to 6.2 kHz were employed.

(31) VanderHart, D. L.; Gutowsky, H. S.; Farrar, T. C. *J. Chem. Phys.* **1969**, *50*, 1058–1065.

(32) Linder, M.; Höhener, A.; Ernst, R. R. *J. Chem. Phys.* **1980**, *73*, 4959–4970.

(33) Zilm, K. W.; Grant, D. M. *J. Am. Chem. Soc.* **1981**, *103*, 2913–2922.

(34) Eichele, K.; Wasylishen, R. E. *J. Magn. Reson., Ser. A* **1994**, *106*, 46–56.

(35) Lumsden, M. D.; Wasylishen, R. E.; Eichele, K.; Schindler, M.; Penner, G. H.; Power, W. P.; Curtis, R. D. *J. Am. Chem. Soc.* **1994**, *116*, 1403–1413.

(36) Wasylishen, R. E.; Penner, G. H.; Power, W. P.; Curtis, R. D. *J. Am. Chem. Soc.* **1989**, *111*, 6082–6086.

(37) Dickson, R. M.; McKinnon, M. S.; Britten, J. F.; Wasylishen, R. E. *Can. J. Chem.* **1987**, *65*, 941–946.

(38) Bryce, D. L.; Bernard, G. M.; Gee, M.; Lumsden, M. D.; Eichele, K.; Wasylishen, R. E. *Can. J. Anal. Sci. Spectrosc.* **2001**, *46*, 46–82.

Spectral simulations were carried out using the programs WSOLIDS¹³⁹ and HBA,⁴⁰ both of which were developed in our laboratory. The HBA program is based on the method of Herzfeld and Berger⁴¹ for the determination of the principal components of chemical shift tensors for spin- $1/2$ nuclei from spectra of MAS samples.

ZORA-DFT Calculations. Indirect nuclear spin–spin coupling tensors were calculated using the CPL coupling module^{42–45} of the Amsterdam density functional program^{46,47} running on an IBM RS6000 workstation or a PC with an AMD Athlon microprocessor. The couplings are calculated on the basis of the spin–orbit relativistic ZORA-DFT implementation of Autschbach and Ziegler.^{42,43} The Fermi-contact (FC), spin-dipolar (SD), and diamagnetic and paramagnetic spin–orbit (DSO and PSO) coupling mechanisms were included in the calculations. All DFT calculations used the VWN⁴⁸ + Becke88⁴⁹ and Perdew86⁵⁰ generalized gradient approximation (GGA).⁴³ The triple-polarized ADF ZORA V Slater-type basis sets available within the ADF package were used on all atoms.

Simple models for the infinite linear chain structure of silver cyanide were used to provide some insight into the dependence of the silver–carbon J coupling on the local structure. To this end, calculations based on the bond lengths reported by Hibble et al.²³ ($r_{\text{AgC}} = r_{\text{AgN}} = 2.06 \text{ \AA}$ and $r_{\text{CN}} = 1.16 \text{ \AA}$) were carried out for the two models shown in Table 1. By calculating the silver–carbon J coupling for these two models, the effect of changing the orientation of the nearest neighbor cyanide moiety may be isolated.

Results and Discussion

Carbon-13 Magic-Angle-Spinning NMR Spectroscopy.

A ^{13}C NMR spectrum of solid $\text{Ag}^{13}\text{C}^{15}\text{N}$ acquired at 4.7 T and with an MAS rate of 6.20 kHz is presented in Figure 1. Under these conditions, direct dipolar coupling interactions between the ^{13}C and $^{109/107}\text{Ag}$ nuclei and between the ^{13}C and ^{15}N nuclei are averaged to zero and do not contribute to the observed spectrum. In combination with other ^{13}C MAS NMR spectra obtained at a variety of MAS rates and field strengths, analysis of this spectrum by the method of Herzfeld and Berger provides the principal components of the carbon chemical shift tensor (Table 2). The axial symmetry of the carbon CS tensor ($\kappa = +1.0$) implies a linear environment at carbon, which is in agreement with the conclusions of Bowmaker²² and of Hibble²³ that silver cyanide exists as infinite linear chains. The principal components of the carbon CS tensor for silver cyanide, $\delta_{\perp} = 276 \pm 2 \text{ ppm}$ and $\delta_{\parallel} =$

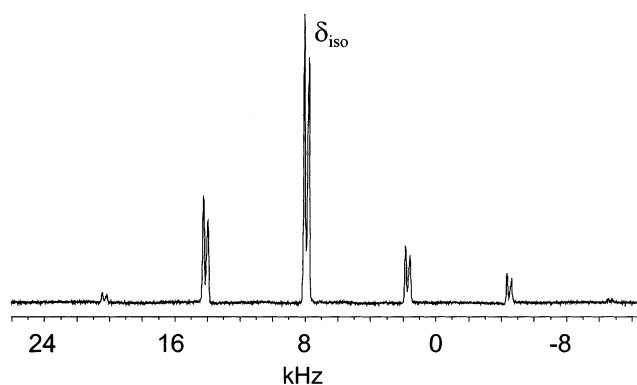


Figure 1. Carbon-13 NMR spectrum of solid ^{13}C - and ^{15}N -enriched (99%) silver cyanide, $\text{Ag}^{13}\text{C}^{15}\text{N}$, acquired at 4.7 T with an MAS rate of 6.20 kHz. The spectrum is the sum of 336 scans acquired with a recycle delay of 200 s. The axial symmetry of the spinning sideband pattern is indicative of the linearity of the AgCN chains. The asymmetric doublet arises as a result of cyanide “head–tail” disorder and indirect nuclear spin–spin coupling to the abundant ^{109}Ag and ^{107}Ag isotopes (see text and Figure 2).

Table 2. Solid-State NMR Results for Silver Cyanide

	carbon	nitrogen
$\delta_{\text{iso}}/\text{ppm}$	157 ± 1^a	249 ± 1
$\delta_{\perp}/\text{ppm}$	276 ± 2	394 ± 2
$\delta_{\parallel}/\text{ppm}$	-79 ± 3	-41 ± 10
$C_Q(^{14}\text{N})/\text{MHz}^b$		-2.9 ± 1.0
$R_{\text{eff}}(^{13}\text{C}, ^{15}\text{N})/\text{Hz}$		-1800 ± 50
$r_{\text{CN}}/\text{\AA}$		1.16 ± 0.03^c

^a Simulations of ^{13}C NMR spectra of stationary samples are based on a one-site model. Simulations of ^{13}C MAS NMR spectra required the use of a two-site model using the data given in Table 3. ^b The electric field gradient asymmetry parameter, η , was set to zero in accordance with the linear geometry of AgCN . ^c See text for a discussion of the corrections made to R_{eff} to obtain this bond length.

$-79 \pm 3 \text{ ppm}$, are identical within error to those reported for copper cyanide, $\delta_{\perp} = 267 \pm 10 \text{ ppm}$ and $\delta_{\parallel} = -84 \pm 10 \text{ ppm}$. The large deshielding perpendicular to the AgCN and CuCN chains is due to paramagnetic contributions to the nuclear magnetic shielding tensor, as discussed for CuCN .²¹

Shown in Figure 2a is the reconstructed isotropic resonance of the spectrum shown in Figure 1; that is, the sidebands have been summed into the centerband to provide the total ^{13}C MAS NMR line shape. The isotropic resonance appears as an asymmetric doublet with an approximate splitting of 280 Hz. To determine the origin of the asymmetric doublet, ^{13}C MAS spectra acquired at 7.05 and 9.4 T were also examined, and it was found that the splitting (in Hz) is field independent and maintains its asymmetry. The fact that it is field independent indicates that the splitting arises because of J coupling between carbon and silver rather than because of significantly different carbon chemical shifts for different sites in AgCN . Indeed, the approximate splitting of 280 Hz is within the typical range observed for one-bond ^{109}Ag – ^{13}C coupling constants, approximately 100–320 Hz.⁵¹

If there were perfect head-to-tail cyanide ordering in AgCN , wherein all cyano moieties are oriented in the same direction (i.e., in a parallel orientation) such that all silver atoms are directly bonded to one carbon atom and one

(39) Eichele, K.; Wasylishen, R. E. *WSOLIDS1 NMR Simulation Package*, version 1.17.30; Dalhousie University and University of Tuebingen: 2001.

(40) Eichele, K.; Wasylishen, R. E. *HBA*, version 1.4.4; Dalhousie University and University of Tuebingen: 2001.

(41) Herzfeld, J.; Berger, A. E. *J. Chem. Phys.* **1980**, *73*, 6021–6030.

(42) Autschbach, J.; Ziegler, T. *J. Chem. Phys.* **2000**, *113*, 936–947.

(43) Autschbach, J.; Ziegler, T. *J. Chem. Phys.* **2000**, *113*, 9410–9418.

(44) Dickson, R. M.; Ziegler, T. *J. Phys. Chem.* **1996**, *100*, 5286–5290.

(45) Khandogin, J.; Ziegler, T. *Spectrochim. Acta* **1999**, *A55*, 607–624.

(46) ADF 2000.01, Theoretical Chemistry, Vrije Universiteit, Amsterdam, <http://www.scm.com>.

(47) (a) Baerends, E. J.; Ellis, D. E.; Ros, P. *Chem. Phys.* **1973**, *2*, 41–51.

(b) Versluis, L.; Ziegler, T. *J. Chem. Phys.* **1988**, *88*, 322–328. (c) te Velde, G.; Baerends, E. J. *J. Comput. Phys.* **1992**, *99*, 84–98. (d) Fonseca Guerra, C.; Snijders, J. G.; te Velde, G.; Baerends, E. J. *Theor. Chim. Acc.* **1998**, *99*, 391–403.

(48) Vosko, S. H.; Wilk, L.; Nusair, M. *Can. J. Phys.* **1980**, *58*, 1200–1211.

(49) Becke, A. D. *Phys. Rev. A* **1988**, *38*, 3098–3100.

(50) Perdew, J. P. *Phys. Rev. B* **1986**, *33*, 8822–8824; **1986**, *34*, 7406.

(51) Zangger, K.; Armitage, I. M. *Metal-Based Drugs* **1999**, *6*, 239–245.

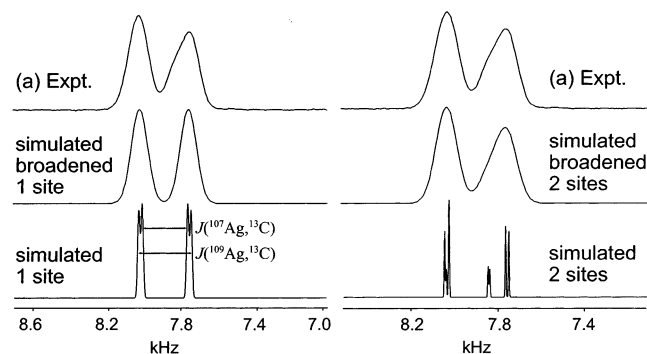


Figure 2. (a) Experimental ^{13}C MAS NMR isotropic resonance (the MAS spinning sidebands have been added to the isotropic centerband as described in the text) for $\text{Ag}^{13}\text{C}^{15}\text{N}$. The simulated isotropic resonance of the ^{13}C MAS NMR spectrum of solid $\text{Ag}^{13}\text{C}^{15}\text{N}$ based on a typical $J_{\text{iso}}(^{109}\text{Ag}, ^{13}\text{C})$ of 280 Hz and the corresponding $J_{\text{iso}}(^{107}\text{Ag}, ^{13}\text{C})$ 243 Hz is shown on the left for a single carbon site. The J coupling between ^{13}C and the two silver isotopes results in four peaks, as shown in the unbroadered spectrum. The asymmetry of the reconstructed experimental isotropic ^{13}C resonance shown in part (a) cannot be reproduced on the basis of a one-site model, as evidenced by the disagreement between the experimental spectrum and the broadened “one-site” simulated spectrum. The simulated isotropic resonances of the ^{13}C MAS NMR spectrum of solid $\text{Ag}^{13}\text{C}^{15}\text{N}$ based on a two-site model, where the isotropic chemical shift and silver–carbon J coupling are slightly different for carbon sites depending on the orientation of the nearest neighbor cyanide ligand, are shown on the right. The experimental spectrum is successfully simulated as the sum of two distinct ^{13}C sites in the approximate ratio 2:1. See text for details.

nitrogen atom (see Table 1), then the experimental spectrum shown in Figure 2 would be successfully reproduced by considering only the carbon isotropic chemical shift and the indirect nuclear spin–spin coupling between ^{13}C and $^{109/107}\text{Ag}$. One-bond coupling constants for ^{13}C and ^{15}N are generally less than 20 Hz in magnitude,^{52–54} and thus, these couplings merely serve to slightly broaden the ^{13}C MAS NMR spectrum. A simulated ^{13}C isotropic resonance based on a single carbon site and a value of 280 Hz for $J(^{109}\text{Ag}, ^{13}\text{C})$ and 243 Hz for $J(^{107}\text{Ag}, ^{13}\text{C})$ (because the magnetogyric ratios of ^{109}Ag and ^{107}Ag are fixed and differ by about 15%) is shown in Figure 2. On the basis of the natural abundances of the spin-active silver isotopes, 48.18% of the ^{13}C nuclei are J coupled to ^{109}Ag , while 51.82% of the ^{13}C nuclei are J coupled to ^{107}Ag . The very similar magnetogyric ratios and natural abundances of ^{109}Ag and ^{107}Ag therefore result in the two almost overlapped doublets of similar intensities shown in the unbroadered simulated one-site spectrum. When this spectrum is broadened, a symmetric doublet is obtained, in disagreement with the experimental spectrum. Reproduction of the asymmetry of the experimental doublet is impossible on the basis of a completely ordered AgCN structure wherein all carbon sites are equivalent.

The experimental isotropic resonance is successfully fit at three applied magnetic field strengths using a two-site model (Figure 2). A two-site model corresponds to the simplest situation, where, for a given Ag–C spin pair, only the orientation of a second nearest-neighbor cyanide ligand

bound to the silver atom significantly influences the NMR spectrum of the ^{13}C nucleus under consideration. This corresponds to the existence of both ordered and disordered sites (see Table 1). This model neglects small longer-range effects on the ^{13}C NMR interaction tensors, such as those induced by interchain translational disorder. Shown in Figure 2 is a simulated unbroadered ^{13}C MAS NMR spectrum based on two sites with approximately identical chemical shifts, 157.0 ppm (site 1) and 157.8 ppm (site 2), and significantly different silver–carbon spin–spin coupling constants. For site 1, $J_{\text{iso}}(^{109}\text{Ag}, ^{13}\text{C})$ is $\pm(297 \pm 15)$ Hz, and for site 2, $J_{\text{iso}}(^{109}\text{Ag}, ^{13}\text{C})$ is $\pm(201 \pm 15)$ Hz (Table 3). The simulation also incorporates $J_{\text{iso}}(^{107}\text{Ag}, ^{13}\text{C})$ coupling, as fixed by the relative magnetogyric ratios of ^{109}Ag and ^{107}Ag . The simulated broadened two-site spectrum shown in Figure 2 agrees with the experimental spectrum only when the two sites are weighted in the ratio $70 \pm 10\%$ (site 1) to $30 \pm 10\%$ (site 2).

The observation of silver–carbon coupling implies silver–carbon connectivity and indicates that the cyanide groups are in a state of static disorder rather than dynamic disorder. That is, any reorientation of CN groups is slow with respect to $1/J_{\text{iso}}(^{109/107}\text{Ag}, ^{13}\text{C})^{-1}$ at room temperature. This conclusion is identical to what has been found for solid CuCN²¹ and contrasts with the situation in solid alkali metal cyanides, where the cyano groups are indeed in a state of dynamic disorder.^{55,56}

Shown in Table 4 are various cyanide ordering scenarios for an “infinite” chain of AgCN. If the cyanide ligands are completely ordered such that all cyanide groups are oriented in the same direction and all silver atoms are bonded to one carbon and one nitrogen (model A), only one type of carbon site would be apparent in the ^{13}C MAS NMR spectrum. Model D features cyanide ligands of alternating orientation such that all silver atoms are in disordered sites and each similarly has only one carbon site which would also give rise to a single resonance in the ^{13}C MAS NMR spectrum. The true percentage of ordered and disordered silver sites therefore lies between these two extremes such that ^{13}C resonances from both NC–Ag–CN and NC–Ag–NC sites have been observed. On the basis of the NMR data, we may conclude that the true ordering scenario is approximately as shown in either model B or C. Here, ratios of 1:2 and 2:1 have been used to represent the two types of carbon sites; this, within experimental error, is what has been observed.

Certainly, $^{109/107}\text{Ag}$ MAS NMR of solid silver cyanide would provide great insight into the nature and distribution of the silver sites. While both silver nuclei are approximately 50% abundant, $^{109/107}\text{Ag}$ NMR of silver cyanide poses several challenges. First, the resonance frequency of ^{109}Ag in a magnetic field of 9.4 T is only 18.7 MHz, resulting in technical difficulties such as probe ringing. Second, the coils in many NMR probes contain silver, thus introducing a

(52) Friesen, K. J.; Wasylishen, R. E. *J. Magn. Reson.* **1982**, *48*, 152–154.

(53) Eichele, K.; Wasylishen, R. E. *Solid State Nucl. Magn. Reson.* **1992**, *1*, 159–163.

(54) Barszczewicz, A.; Helgaker, T.; Jaszuński, M.; Jørgensen, P.; Ruud, K. *J. Magn. Reson., Ser. A* **1995**, *114*, 212–218.

(55) Wasylishen, R. E.; Jeffrey, K. R. *J. Chem. Phys.* **1983**, *78*, 1000–1002.

(56) Wasylishen, R. E.; Pettitt, B. A.; Jeffrey, K. R. *J. Chem. Phys.* **1981**, *74*, 6022–6026.

Table 3. Experimental and Calculated Silver–Carbon Indirect Nuclear Spin–Spin Coupling Constants, $^1J_{\text{iso}}(^{109}\text{Ag}, ^{13}\text{C})/\text{Hz}$ for Silver Cyanide

	$^1J_{\text{iso}}(^{109}\text{Ag}, ^{13}\text{C})/\text{Hz}$		difference in $^1J_{\text{iso}}(^{109}\text{Ag}, ^{13}\text{C})/\text{Hz}$
^{13}C MAS NMR	(–)297 ± 15 (site 1)	(–)201 ± 15 (site 2)	96 ± 30
ZORA-DFT	–308 (model I)	–234 (model II average ^a)	74

^a This represents the average J coupling for both carbon nuclei coupled to silver in model II.

Table 4. Cyanide “Head–Tail” Ordering in Silver Cyanide

model	% of ^{13}C NMR-active silver sites ^a		
	C–Ag–C	C–Ag–N	% Ag in disordered sites ^b
A	0	100	0
B	33	66	33
C	66	33	66
D	100	0	100 ^c

^a The percentages listed here are attributable to the total number of silver sites which may be probed by NMR observation of directly bonded ^{13}C nuclei. Therefore, the disordered “–N–Ag–N–” sites are unavoidably not included in these percentages. ^b The percentages listed here are attributable to the total number of silver sites. ^c As mentioned in Table 1, model D may be considered as an arrangement of perfectly antiparallel-ordered silver cyanide; however, in the present work we use the definitions of “ordered” and “disordered”, as shown in Table 1, to refer to the silver environments. Therefore, it is true that 100% of the silver sites are in disordered environments.

background signal into the spectrum. The opportunity for cross-polarization, an extremely beneficial technique in the acquisition of solid-state NMR spectra of dilute spin- $1/2$ nuclei, from protons to silver,^{57,58} does not exist because of the absence of protons in AgCN. An additional expected complication for silver cyanide is a particularly anisotropic silver CS tensor, which will cause the intensity of the ^{109}Ag MAS NMR spectrum to be distributed over a large spectral width. Finally, the spin–lattice relaxation time constant T_1 of $^{109/107}\text{Ag}$ nuclei may be extremely large in many cases;⁵⁹ for example, the $T_1(^{109}\text{Ag})$ of silver nitrate solution is nearly 20 min!^{60,61} The $T_1(^{109}\text{Ag})$ in solid silver nitrate is at least on the order of hours and may be much longer.⁶² For all of these reasons, $^{109/107}\text{Ag}$ MAS NMR spectra of solid AgCN remain elusive, despite many attempts to record such spectra at a variety of applied magnetic field strengths.

To distinguish between models B and C, we make use of the fact that the experimental values of $J_{\text{iso}}(^{109/107}\text{Ag}, ^{13}\text{C})$ are significantly different for site 1 and site 2. For this purpose, relativistic ZORA-DFT calculations have been carried out on simple fragments to model ordered (model I) and disordered (model II) sites (see Table 1). The results are summarized in Table 3. The calculations do not produce quantitative agreement with the experiment because of the well-known difficulties associated with calculating \mathbf{J} tensors as well as the simplicity of the model systems. Nevertheless, the calculated magnitudes of $^1J_{\text{iso}}(^{109}\text{Ag}, ^{13}\text{C})$ are well within

the known experimental range, and the *difference* in the spin–spin coupling constants for an ordered site and a disordered site, 74 Hz, is in good agreement with the experimental value of 96 ± 30 Hz. Site 1 from the ^{13}C MAS NMR simulations may be assigned to model I from the ZORA-DFT calculations, and site 2 may be assigned to model II. Thus, we conclude that model B shown in Table 4 is in best agreement with the ^{13}C MAS NMR data. Model B features 33% of all silver atoms in disordered sites, that is, either –NC–Ag–CN– or –CN–Ag–NC–. This is an identical result to what was obtained in solid copper cyanide.²¹ If the cyanide ordering were completely random, one would expect 50% of the silver atoms to occupy disordered sites; thus, it may be concluded that there is a measurable preference for the cyanide groups to be ordered.

On the basis of the ^{13}C NMR parameters determined from the analysis of $\text{Ag}^{13}\text{C}^{15}\text{N}$ described above, a successful simulation of ^{13}C MAS NMR spectra of $\text{Ag}^{13}\text{C}^{14}\text{N}$ was also possible. For the latter isotopomer, residual dipolar coupling between ^{13}C and the quadrupolar ^{14}N nucleus²⁶ contributes to the ^{13}C MAS NMR spectrum in addition to the silver–carbon spin–spin coupling interactions described above for $\text{Ag}^{13}\text{C}^{15}\text{N}$. While the experimental uncertainties in $^1J_{\text{iso}}(^{109/107}\text{Ag}, ^{13}\text{C})$ and the relative intensities of site 1 and site 2 preclude an extremely precise measurement of the ^{14}N nuclear quadrupolar coupling constant, a value of -2.9 ± 1.0 MHz may nevertheless be extracted from spectral simulations. This may be compared, for example, to the value 2.284 MHz reported for the cyanate nitrogen in solid ammonium thiocyanate.³⁷ The asymmetry parameter, η , of the ^{14}N electric field gradient tensor in AgCN was set to zero in accordance with the axial symmetry observed for both carbon and nitrogen (vide infra) CS tensors.

Nitrogen-15 NMR Spectroscopy. Presented in Figure 3 is an ^{15}N MAS NMR spectrum of solid ^{15}N -enriched (99%) silver cyanide. In combination with other ^{15}N NMR spectra of static and MAS samples obtained at 4.7 and 9.4 T,

- (57) (a) Sebald, A. *NMR: Basic Princ. Prog.* **1994**, *31*, 91–131. (b) Merwin, L. H.; Sebald, A. *J. Magn. Reson.* **1992**, *97*, 628–631.
 (58) Fijolek, H. G.; Oriskovich, T. A.; Benesi, A. J.; González-Duarte, P.; Natan, M. J. *Inorg. Chem.* **1996**, *35*, 797–799.
 (59) Henrichs, P. M. In *NMR of Newly Accessible Nuclei, Volume 2—Chemically and Biochemically Important Elements*; Laszlo, P., Ed.; Academic Press: New York, 1983; Chapter 12.
 (60) Pfister, H.; Schwenk, A.; Zeller, D. *J. Magn. Reson.* **1986**, *68*, 138–145.
 (61) Granger, P. In *Studies in Inorganic Chemistry, Volume 13—Transition Metal Nuclear Magnetic Resonance*; Pregosin, P. S., Ed.; Elsevier: Amsterdam, 1991; pp 273–288.
 (62) Moudrakovski, I. Personal communication.

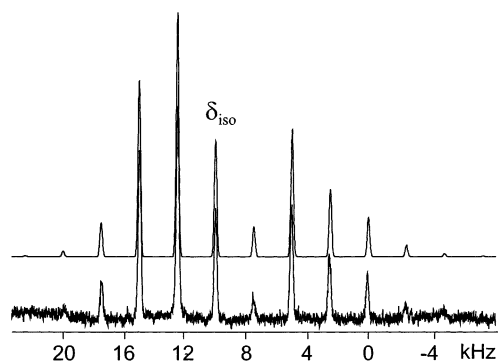


Figure 3. Nitrogen-15 NMR spectrum of solid ^{15}N -enriched (99%) silver cyanide, AgC^{15}N , acquired at 9.4 T with an MAS rate of 2.52 kHz. The spectrum is the sum of 459 scans acquired with a recycle delay of 200 s. The axial symmetry of the spinning sideband pattern is indicative of the linearity of the AgCN chains. Also shown is the best-fit simulated spectrum based on the nitrogen chemical shift tensor parameters given in Table 2.

simulation of the spectrum via a Herzfeld–Berger analysis provides the principal components of the nitrogen CS tensor as $\delta_{\perp} = 394 \pm 2$ ppm and $\delta_{\parallel} = -41 \pm 10$ ppm. As for the carbon CS tensor parameters, those of nitrogen are similar to the results reported for solid CuCN , $\delta_{\perp} = 385 \pm 10$ ppm and $\delta_{\parallel} = -70 \pm 10$ ppm. The axial symmetry of the nitrogen CS tensor provides further evidence for linearity at nitrogen in the AgCN chains. Line widths in the ^{15}N MAS spectra on the order of 250 Hz at 9.4 T allude to the possibility of $^{109/107}\text{Ag}, ^{15}\text{N}$ J coupling; however, no such couplings are resolved. This observation is consistent with the fact that typical one-bond $^{109}\text{Ag}, ^{15}\text{N}$ J couplings are rather small and fall in the range from 12 to 57 Hz.^{61,63,64} Additional broadening may also arise because of the cyanide “head–tail” disorder discussed above; however, neither the chemical shift difference between different nitrogen sites nor the $J(^{109/107}\text{Ag}, ^{15}\text{N})$ coupling is sufficiently large to induce a resolved splitting in the ^{15}N spectrum. This is true of spectra acquired at both 4.7 and 9.4 T. Since the line widths in NMR spectra of solids typically scale with B_0 , J coupling would be more easily observed at lower field strengths, while chemical shift differences would be amplified at higher field strengths.

Carbon-13 Dipolar–Chemical Shift NMR Spectroscopy. Shown in Figure 4 is a ^{13}C NMR spectrum of a stationary powder sample of $\text{Ag}^{13}\text{C}^{15}\text{N}$ (99%) obtained at 7.05 T. To efficaciously interpret this dipolar–CS spectrum, the relative magnitudes of several spin–spin coupling interactions involving ^{13}C must be considered. The relevant interactions are $^{109/107}\text{Ag}, ^{13}\text{C}$ direct dipolar coupling, $^1J_{\text{iso}}(^{109,107}\text{Ag}, ^{13}\text{C})$ coupling, $^{15}\text{N}, ^{13}\text{C}$ dipolar coupling, and $^1J_{\text{iso}}(^{15}\text{N}, ^{13}\text{C})$ coupling. Employing silver–carbon direct dipolar coupling constants ($R_{\text{DD}}(^{109}\text{Ag}, ^{13}\text{C}) = -162$ Hz and $R_{\text{DD}}(^{107}\text{Ag}, ^{13}\text{C}) = -141$ Hz) based on the bond lengths reported by Hibble²³ and a $^1J_{\text{iso}}(^{109,107}\text{Ag}, ^{13}\text{C})$ of -250 Hz, simulations of ^{13}C powder patterns indicate that these

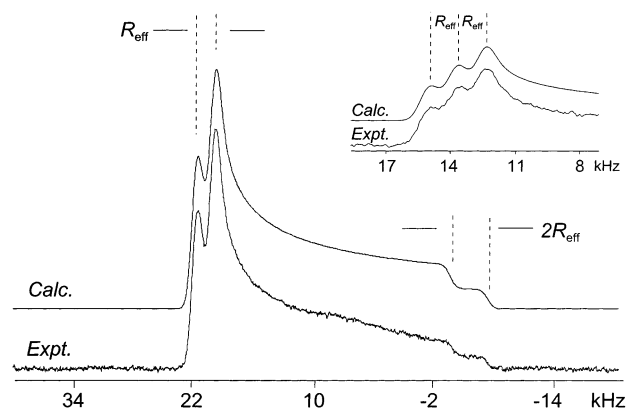


Figure 4. Carbon-13 NMR spectrum of a stationary sample of solid ^{13}C - and ^{15}N -enriched (99%) silver cyanide, $\text{Ag}^{13}\text{C}^{15}\text{N}$, acquired at 7.05 T. The spectrum is the sum of 733 scans acquired with a recycle delay of 120 s. The axial symmetry of the powder pattern is indicative of the linearity of the AgCN chains. Splittings due to direct dipolar coupling between ^{13}C and ^{15}N are indicated. Also shown is the best-fit simulated spectrum. Shown in the inset are the high-frequency discontinuities of the ^{13}C NMR spectrum of a stationary sample of solid ^{13}C -enriched (99%) silver cyanide, $\text{Ag}^{13}\text{C}\text{N}$, acquired at 4.7 T. Splittings due to direct dipolar coupling between ^{13}C and ^{14}N are indicated. Also shown is the best-fit simulated spectrum.

relatively small interactions will merely serve to broaden each of the ^{13}C subspectra associated with dominant direct dipolar coupling to the ^{15}N nucleus. As mentioned above, $^1J_{\text{iso}}(^{15}\text{N}, ^{13}\text{C})$ is typically on the order of 10 Hz and as such will not make any noticeable impact on the ~ 30 kHz-wide static ^{13}C NMR line shape.

The ^{13}C NMR spectrum presented in Figure 4 may therefore be properly analyzed on the basis of the assumption of an effectively “isolated” ^{13}C – ^{15}N spin pair, with the silver–carbon spin–spin coupling interactions resulting in a broadening of the discontinuities in the spectrum but without affecting the magnitude of the splitting due to ^{15}N .

The effective dipolar coupling between ^{13}C and ^{15}N manifests itself as a splitting R_{eff} at the high-frequency side of the powder pattern and $2R_{\text{eff}}$ at the low-frequency side.³⁷ In ^{13}C NMR spectra of stationary samples of $\text{Ag}^{13}\text{C}^{14}\text{N}$ (see inset of Figure 4), the dipolar splitting between ^{13}C and the 99.6% abundant ^{14}N nucleus manifests itself in a similar manner; however, the powder pattern is split into three rather than two because of the three allowed spin states of ^{14}N . In combination with the CS tensor parameters measured from MAS samples, the spectra shown in Figure 4 may be successfully simulated to extract the effective ^{13}C – ^{15}N dipolar coupling constant. The accuracy and precision of the final reported value of $R_{\text{eff}}(^{13}\text{C}, ^{15}\text{N})$, -1800 ± 50 Hz (Table 2), are based on simulations of ^{13}C NMR spectra of stationary samples of both $\text{Ag}^{13}\text{C}^{15}\text{N}$ and $\text{Ag}^{13}\text{C}^{14}\text{N}$ obtained at multiple field strengths. The agreement in values of $R_{\text{eff}}(^{13}\text{C}, ^{15}\text{N})$ determined from the splittings in the ^{13}C spectra of both $\text{Ag}^{13}\text{C}^{15}\text{N}$ and $\text{Ag}^{13}\text{C}^{14}\text{N}$ further demonstrates the validity of treating the system as an AX spin pair.

Determination of a carbon–nitrogen bond length from the measured value of R_{eff} necessitates a detailed discussion of the factors which will affect the accuracy of the final result. As mentioned in the Theory section, two factors exist which must be considered when converting a measured effective dipolar coupling constant to a bond length: (i) the value of

(63) van Stein, G. C.; van Koten, G.; Vrieze, K.; Brevard, C.; Spek, A. L. *J. Am. Chem. Soc.* **1984**, *106*, 4486–4492.

(64) Berger, S.; Braun, S.; Kalinowski, H.-O. *NMR Spectroscopy of the Non-Metallic Elements*; John Wiley & Sons: Chichester, 1997; Chapter 4.

ΔJ and (ii) the extent to which motional averaging affects the dipolar coupling constant. An experimental liquid crystal NMR investigation of methyl isocyanide, $\text{H}_3\text{C}-\text{NC}$, provides a value of -60.0 ± 3.9 Hz for $\Delta J(^{13}\text{C}, ^{15}\text{N})$ for the cyano group.⁶⁵ Multiconfigurational self-consistent field calculations of $\Delta J(^{13}\text{C}, ^{15}\text{N})$ for the cyano groups in HCN, CH_3CN , HNC, and CH_3NC range from -47.1 to -54.6 Hz.⁵⁴ The ZORA-DFT calculations on models I and II (Table 1) provide a value of -42 Hz. Thus, it is reasonable to suggest an upper limit of approximately -60 Hz for $\Delta J(^{13}\text{C}, ^{15}\text{N})$ in silver cyanide. This corresponds to a maximum contribution to R_{eff} of 1% and a maximum error in the determination of the value of r_{CN} of about 0.3% or 0.004 \AA . Clearly, ΔJ will not be a major source of uncertainty in the final value of r_{CN} .

Accounting for the effects of motional averaging is less straightforward. Nevertheless, motional averaging will inevitably result in a reduction in R_{DD} and a corresponding apparent increase in r_{CN} (cf. eq 1).⁶⁶ Before considering the effects of motional averaging in detail, it is therefore possible to place an upper limit on the value of r_{CN} by applying eq 1 directly. Using $R_{\text{eff}} = -1800$ Hz and neglecting ΔJ , an upper limit value of $r_{\text{CN}} = 1.194 \text{ \AA}$ is obtained.

Bond lengths obtained from room-temperature NMR experiments are known to be 1–4% larger than those obtained from X-ray or neutron diffraction experiments.^{66–69} While molecular “stretching” vibrations contribute in part to a partial averaging of the direct dipolar interaction, bending and torsional librations are primarily responsible. Incorporation of librational effects increases the accuracy but reduces the precision of the NMR result. Starting with the experimental value $R_{\text{eff}} = -1800 \pm 50$ Hz, incorporating a value of -60 Hz for ΔJ , and making a librational correction of $2.5 \pm 1.5\%$ to r_{CN} , the observed NMR result from the present work is $r_{\text{CN}} = 1.16 \pm 0.03 \text{ \AA}$. This result is in agreement with the recent neutron diffraction value of Hibble et al., 1.16 \AA .²³

(65) Hiltunen, Y.; Jokisaari, J.; Lounila, J.; Pulkkinen, A. *J. Am. Chem. Soc.* **1989**, *111*, 3217–3220.

(66) Ishii, Y.; Terao, T.; Hayashi, S. *J. Chem. Phys.* **1997**, *107*, 2760–2774.

(67) Carravetta, M.; Eden, M.; Johannessen, O. G.; Luthman, H.; Verdegem, P. J. E.; Lugtenburg, J.; Sebald, A.; Levitt, M. H. *J. Am. Chem. Soc.* **2001**, *123*, 10628–10638.

(68) Ishii, Y. *J. Chem. Phys.* **2001**, *114*, 8473–8483.

(69) Case, D. A. *J. Biomol. NMR* **1999**, *15*, 95–102.

Conclusions

Solid-state ^{13}C and ^{15}N NMR spectroscopy of several isotopomers of silver cyanide has provided unique insights into its structure. The NMR experiments have provided information in agreement with and complementary to the recent total neutron diffraction study of Hibble and co-workers.

The axial symmetry of carbon and nitrogen chemical shift tensors provides evidence for linearity in the structure of AgCN. Carbon-13 MAS NMR spectra, in combination with relativistic ZORA-DFT calculations, indicate that the cyanide ligands in AgCN do not align themselves in a completely random fashion but rather express a measurable preference for parallel cyanide ordering. The number of silver atoms that reside in disordered sites of the types $-\text{NC}-\text{Ag}-\text{CN}-$ and $-\text{CN}-\text{Ag}-\text{NC}-$ is $30 \pm 10\%$. This is in complete analogy with the situation in solid copper cyanide.

Carbon-13 NMR spectroscopy of stationary samples of silver cyanide provides an upper limit on the carbon–nitrogen bond length, r_{CN} , of 1.194 \AA . After accounting for anisotropic J coupling and, more importantly, the effects of librational averaging on the NMR bond length, a more accurate NMR result of $1.16 \pm 0.03 \text{ \AA}$ is obtained. This is in agreement with the result of Hibble.²³

The present work demonstrates the ability of multinuclear magnetic resonance spectroscopic investigations to provide information on disordered and amorphous materials which are not easily studied by conventional diffraction methods. In cases where diffraction data are available, NMR has the potential to provide complementary novel information from a different perspective.

Acknowledgment. The authors thank Kris Harris, Dr. Igor Moudrakovski, and Professor Scott Kroeker for helpful discussions. We thank Dr. Jim Frye and Professor Glenn Penner for valiant efforts to obtain ^{109}Ag MAS NMR spectra of silver cyanide. We thank the Natural Sciences and Engineering Research Council (NSERC) of Canada for research grants. R.E.W. is a Canada Research Chair in Physical Chemistry at the University of Alberta and thanks the University of Alberta for support. D.L.B. thanks NSERC, Dalhousie University, the Izaak Walton Killam Trust, and the Walter C. Sumner Foundation for postgraduate scholarships.

IC0201553